IPHO-Journal of Advance Research in Applied Science
(e-ISSN 3050-8835, p-ISSN 3050-9289 | www.iphopen.org)
Peer-Reviewed | Open Access | Indexed Internationally
Vol. 03, Issue 08, August 2025 | Pages: 01–23 Article ID: 327

DOI: https://doi.org/10.5281/zenodo.16917059

IPHO-Journal of Advance Research in Applied Science
E-ISSN 3050-8835 P-ISSN 3050-9289

Properties, actuarial measures and data modelling applications of the new heavy-tailed Kumaraswamy half-logistic-G family of distributions

Takesure Nyakuamba[1], Joseph Manyemba[1], Norah Chishamiso Gwesu[2], Luba Gilberta Thwala[3], Rita Sauriri[4] and Wilbert Nkomo[1*]

[1]Department of Applied Statistics, Manicaland State University of Applied Sciences, Zimbabwe.
[2]Department of Accounting, Manicaland State University of Applied Sciences, Zimbabwe.
[3]Department of Mining and Mineral Processing Engineering, Manicaland State University of Applied Sciences, Zimbabwe.
[4]Department of Tourism, Hospitaity and Leisure Science, Manicaland State University of Applied Sciences, Zimbabwe.

Abstract

This study introduces the Heavy-Tailed Kumaraswamy Half-Logistic-G family of distributions, a flexible statistical framework for modeling data with heavy-tailed behavior. The research explores its mathematical properties, estimation via maximum likelihood, and performance in actuarial risk assessment. Monte Carlo simulations verify the consistency of parameter estimates, while numerical analyses evaluate some key risk measures, demonstrating the model's effectiveness in extreme-value modeling. A special case, the Heavy-Tailed Kumaraswamy Half-Logistic-Weibull distribution, is compared with relevant competing heavy-tailed models, proving its superior adaptability and precision. Real-world applications further validate its practicality in capturing complex data patterns. The findings highlight the model's robustness and relevance in actuarial science, finance, and risk analysis, offering a powerful

tool for researchers and practitioners. By combining theoretical rigor, computational validation, and empirical evidence, this work advances statistical distribution theory and enhances modeling capabilities for heavy-tailed phenomena.

Keywords: Kumaraswamy-G, Heavy-tail-G, half logistic distribution, estimation, moments, risk measures
Mathematics Subject Classification: 62E99, 60E05

1 Introduction

In applied research, the analysis of empirical data plays a pivotal role in uncovering underlying patterns and forecasting critical phenomena. Lifespan data in particular, contain substantial information that must be accurately modeled to detect significant trends and extreme events. However, conventional probability distributions frequently prove inadequate in capturing the complexity of real-world data across disciplines such as finance, medical sciences, environmental studies, engineering, and economics. This limitation has motivated the development of generalized families of distributions, which enhance flexibility and improve statistical modeling.

Recent advances in distribution theory have led to the introduction of numerous extended families of distributions, designed to address the shortcomings of classical models. Notable contributions include the type I heavy-tailed pioneered by Zhao et al. (2020), the gamma Topp-Leone type II exponentiated half logistic proposed by Oluyede and Moakofi (2023), Kumaraswamy Weibull by Cordeiro, Ortega and Nadarajah (2010), Topp-Leone heavy-tailed type II exponentiated half logistic-G family of distributions (FoDs) by Nkomo, Oluyede and Chipepa (2025), generalized odd Maxwell-Kumaraswamy distribution by Ishaq et al. (2024), Marshall-Olkin-Kumaraswamy-G FoDs developed by Handique, Chakraborty and Hamedani (2017), Topp-Leone type I heavy-tailed-G power series class of distributions by Nkomo, Oluyede and Chipepa (2025), among others. These generalized frameworks exhibit greater adaptability, improved tail behavior, and enhanced fitting capabilities, making them indispensable in modern statistical applications.

This study contributes to this evolving field by introducing the new Heavy-Tailed Kumaraswamy Half-Logistic-G (HT-K-HL-G) FoDs, designed to improve modeling accuracy in risk assessment and extreme-value analysis. By integrating flexible parameterization and heavy-tailed properties, the proposed family offers a powerful alternative to existing models, particularly in reliability, bio-medical sciences, financial risk modeling, among other fields.

In their study, Cordeiro and Castro (2011) introduced the Kumaraswamy-G FDs a flexible and valuable tool for modeling data bounded on the interval

[0,1]. It features closed-form expressions for its cumulative and probability density functions, facilitating straightforward computations and statistical inference. The Kumaraswamy-G FDs cumulative distribution function (cdf) is

$$F(x;\alpha,\beta,\Phi) = 1-[1-(G(x;\Phi))^{\alpha}]^{\beta} \tag{1}$$

and probability distribution function (pdf) is

$$f(x;\alpha,\beta,\Phi) = \alpha\beta g(x;\Phi)\left(G(x;\Phi)\right)^{\alpha-1}\left[1-(G(x;\Phi))^{\alpha}\right]^{\beta-1}, \tag{2}$$

where $G(x;\Phi)$ and $g(x;\Phi) = \frac{dG(x;\Phi)}{dz}$ are the cdf and pdf of the parent distribution respectively, Φ is the parent distribution vector of parameters, and α and β are two positive shape parameters.

The type I half-logistic FoDs pioneered by Cordeiro Alizadeh and Marinho (2016) has cdf

$$\begin{aligned} F(x;\rho,\Phi) &= \int_0^{-\ln(1-G(x;\Phi))} \frac{2\rho\exp(-\rho x)}{1+\exp(-\rho x)}dx \\ &= \frac{1-[1-G(x;\Phi)]^{\rho}}{1+[1-G(x;\Phi)]^{\rho}}, \end{aligned} \tag{3}$$

where $\rho > 0$ is a shape parameter. If we set $\rho = 1$ in Equation (3), then the type I half logistic FoDs reduces to half-logistic-G FoDs , with cdf

$$F(x;\Phi) = \frac{G(x;\Phi)}{1+\bar{G}(x;\Phi)} \tag{4}$$

and pdf

$$f(x;\Phi) = \frac{2g(x;\Phi)}{(1+\bar{G}(x;\Phi))^2}. \tag{5}$$

Note that, $\bar{G}(x;\Omega) = 1-G(x;\Omega)$. Extensions of the half-logistic distribution generate a class of versatile statistical distributions capable of robustly fitting datasets with varying skewness and kurtosis profiles. These distributions enhance modeling adaptability, making them particularly useful in applied contexts.

Replacing the baseline cdf in Equation (1) by the cdf in Equation (4) yields the Kumaraswamy half-logistic (K-HL-G) FoDs with cdf and pdf given by

$$F(x;\alpha,\beta,\Phi) = 1-\left[1-\left(\frac{G(x;\Phi)}{1+\bar{G}(x;\Phi)}\right)^{\alpha}\right]^{\beta} \tag{6}$$

and

$$f(x;\alpha,\beta,\Phi) = \frac{2\alpha\beta g(x;\Phi)(G(x;\Phi))^{\alpha-1}}{(1+\bar{G}(x;\Phi))^{\alpha-1}}, \quad (7)$$

respectively, where $\alpha, \beta > 0$ are both shape parameters.

In this research, we propose a new FoDs, termed the Heavy-Tailed Kumaraswamy Half-Logistic-G (HT-K-HL-G) FoDs, which exhibits remarkable flexibility in data fitting, as demonstrated by its capacity to capture diverse density and hazard rate shapes across its special cases. The development of this framework is motivated by several key objectives:

(i) Unifying the heavy-tailed-G, Kumaraswamy-G, and half-logistic-G families to enhance modeling flexibility of existing distribution frameworks;

(ii) Broadening the spectrum of possible parent density and hazard rate functions to accommodate more complex data structures;

(iii) Constructing heavy-tailed distributions capable of effectively modeling real-world datasets from diverse application domains;

(iv) Assessing the efficacy of the HT-K-HL-G FoDs in characterizing risk measures, thereby supporting robust decision-making and advanced risk management methodologies.

The following describes how the paper is structured. We develop the new FoDs in Section 2. In Section 3, statistical properties and special cases for specified baseline distributions are discussed. We discuss risk measures in Section 4. We conduct the estimation of parameters in Section 5. Section 6 of the study is dedicated to presenting the results of the simulations conducted. In Section 7, data examples are provided, and the concluding observations of the research are presented in Section 8.

2 The New FoDs and its Properties

Zhao et al. (2020) proposed the heavy-tailed-G (HT-G) FoDs with cdf

$$F(x;\theta,\Phi) = 1 - \left(\frac{\bar{G}(x;\Phi)}{1-(1-\theta)G(x;\Phi)}\right)^{\theta} \quad (8)$$

and pdf

$$f(x;\theta,\Phi) = \frac{\theta^2 g(x;\Phi)\left[\bar{G}(x;\Phi)\right]^{\theta-1}}{\left[1-(1-\theta)G(x;\Phi)\right]^{\theta+1}}, \quad (9)$$

where $\theta > 0$ is both a shape and tilt parameter. Replacing the baseline cdf in Equation (8) with the K-HL-G cdf yields the HT-K-HL-G FoDs. The cdf, survival function and pdf are given by

$$F(x;\theta,\alpha,\beta,\Phi) = 1-\left(\frac{\left[1-\left(\frac{G(x;\Phi)}{1+\bar{G}(x;\Phi)}\right)^{\alpha}\right]^{\beta}}{1-(1-\theta)\left[1-\left(\frac{G(x;\Phi)}{1+\bar{G}(x;\Phi)}\right)^{\alpha}\right]^{\beta}}\right)^{\theta}, \quad (10)$$

$$S(x;\theta,\alpha,\beta,\Phi) = \left(\frac{\left[1-\left(\frac{G(x;\Phi)}{1+\bar{G}(x;\Phi)}\right)^{\alpha}\right]^{\beta}}{1-(1-\theta)\left[1-\left(\frac{G(x;\Phi)}{1+\bar{G}(x;\Phi)}\right)^{\alpha}\right]^{\beta}}\right)^{\theta} \quad (11)$$

and

$$\begin{aligned} f(x;\theta,\alpha,\beta,\Phi) &= 2\alpha\theta^2\beta g(x;\Phi)\left(\frac{G(x;\Phi)}{1+\bar{G}(x;\Phi)}\right)^{\alpha-1}\left[1-\left(\frac{G(x;\Phi)}{1+\bar{G}(x;\Phi)}\right)^{\alpha}\right]^{\beta\theta-1} \\ &\times \left[1-(1-\theta)\left[1-\left(\frac{G(x;\Phi)}{1+\bar{G}(x;\Phi)}\right)^{\alpha}\right]^{\beta}\right]^{-(\theta+1)}, \end{aligned} \quad (12)$$

respectively, where $x,\theta,\alpha,\beta > 0$. The hazard rate function (hrf) of the HT-K-HL FoDs is

$$\begin{aligned} h(x;\theta,\alpha,\beta,\Phi) &= 2\alpha\theta^2\beta g(x;\Phi)\left(\frac{G(x;\Phi)}{1+\bar{G}(x;\Phi)}\right)^{\alpha-1}\left[1-\left(\frac{G(x;\Phi)}{1+\bar{G}(x;\Phi)}\right)^{\alpha}\right]^{-1} \\ &\times \left[1-(1-\theta)\left[1-\left(\frac{G(x;\Phi)}{1+\bar{G}(x;\Phi)}\right)^{\alpha}\right]^{\beta}\right]^{-1)}. \end{aligned} \quad (13)$$

It is important to note that various sub-families HT-K-HL FoDs can be found by setting individual parameters to unit.

3 Statistical and Mathematical Properties

The mathematical and statistical properties of probability distributions are essential because they characterize the behavior of random variables, enabling predictions, hypothesis testing, and decision-making in various domains. These properties ensure that models accurately represent real-world uncertainty and allow for meaningful statistical inference.

3.1 Density function series expansion

The pdf of the new HT-K-HL-G FoDs can be written as

$$f(x;\theta,\alpha,\beta,\Phi) = \sum_{l=0}^{\infty} \Theta_{l+1} g_{l+1}(x;\Phi),$$

where $g_{l+1}(x;\Phi) = (l+1)g(x;\Phi)G^{l}(x;\Phi)$ is the exponentiated-G (Expo-G) distribution with power parameter $(l+1)$ and

$$\begin{aligned}\Theta_{l+1} &= 2\alpha\theta^{2}\beta \sum_{h,i,j,k,l=0}^{\infty} \frac{(-1)^{i+j+k}}{l+1}(1-\theta)^{h}\binom{\theta+h}{h}\binom{\beta(h+\theta)-1}{i} \\ &\times \binom{\alpha(i+1)-1}{j}\binom{\alpha(i+1)+k}{k}\binom{j+k}{l}, \end{aligned} \tag{14}$$

is the linear component. Therefore, the HT-K-HL-G FoDs is expressible as an infinite linear combination of the exponentited-G (Expo-G) densities from which we can directly derive other statistical properties. Detailed derivations of the density expansion are provided in the **web appendix**.

3.2 Quantile function

The quantile of the new HT-K-HL-G FoDs is

$$Q_X(u) = G^{-1}\left(\frac{\left(1-\left[\frac{(1-(1-\theta)u^{1/\theta})}{1-(1-\theta)u^{1/\theta}+u^{1/\theta}}\right]^{1/\beta}\right)^{1/\alpha}}{1+\left(1-\left[\frac{(1-(1-\theta)u^{1/\theta})}{1-(1-\theta)u^{1/\theta}+u^{1/\theta}}\right]^{1/\beta}\right)^{1/\alpha}}\right), \tag{15}$$

where $u \in [0,1]$ for $\theta,\alpha,\beta > 0$. Consequently, the quantile values can be obtained by utilizing R software to solve the non-linear equation. The inverse baseline cdf $G^{-1}(.)$ must be known for implementation. For simulations or statistical applications, this quantile function enables random variate generation via the inverse transform method..

3.3 Moments and incomplete moments

If Y_{l+1} is an Expo-G distributed random variable with power parameter $(l+1)$, then the q^{th} moment of the new FoDs is

$$E(X^{q}) = \sum_{r=0}^{\infty} \Theta_{l+1} E(Y_{l+1}^{q}),$$

where Θ_{l+1} is specified in Equation (14) and $E(Y_{l+1}^q)$ is the q^{th} moment of Y_{l+1}. The q^{th} incomplete moment is

$$I_X(t) = \int_0^t x^q f(x)dx = \sum_{l=0}^{\infty} \Theta_{l+1} I_{l+1}(t; q, \Phi),$$

where $I_{l+1}(t; p, \Phi) = \int_0^t x^q g_{l+1}(x; \Phi)dx$ represents the incomplete moment of Y_{l+1}. The moment generating function (MGF) of X is

$$M_X(t) = \sum_{l=0}^{\infty} \Theta_{l+1} E(e^{tY_{l+1}}),$$

where $E(e^{tY_{l+1}})$ is the MGF of Y_{l+1} and Φ_{l+1} is specified in Equation (14).

Incomplete moments are crucial in the construction of Bonferroni and Lorenz curves for the HT-K-HL-G FoDs, while complete moments are valuable in the computation of coefficients of variation, skewness, kurtosis, and other related characteristics.

3.4 Order statistics

The form of the pdf of the h^{th} order statistic from the HT-K-HL-G FoDs is

$$\begin{aligned} f_{h:n}(x) &= \frac{f(x)}{B(h, n-h+1)} \sum_{j=0}^{n-h} \binom{n-h}{j} [F(x)]^{j+h-1} \\ &= \frac{1}{B(h, n-h+1)} \sum_{z=0}^{\infty} \sum_{j=0}^{n-h} \binom{n-h}{j} \Psi_{v+1} g_{v+1}(x; \Phi), \end{aligned}$$

where $B(.,.)$ is the beta function, $g_{v+1}(x; \Phi) = (v+1)g(x; \Phi)G^v(x; \Phi)$ is the Expo-G distribution with power parameter $(v+1)$ and

$$\begin{aligned} \Psi_{v+1} &= 2\alpha\theta^2\beta \sum_{q,r,s,t,u=0}^{\infty} (-1)^{q+s+t+u+v} (1-\theta)^r \binom{+h-1}{q} \binom{\theta(q+1)+r}{r} \\ &\times \binom{\beta[\theta(q+1)+r]-1}{s} \binom{\alpha(s+1)-1}{t} \binom{\alpha(s+1)+u}{u} \binom{t+u}{v} \left(\frac{1}{v+1}\right). \end{aligned}$$

In light of this, we draw the conclusion that the pdf of the h^{th} order statistic from the HT-K-HL-G FoDs can be expressed as an infinite linear combination of the Expo-G densities. The **web appendix** contains detailed derivations.

3.5 Entropy

Entropy quantifies the level of indeterminacy inherent in a probability distribution. The two widely used measures of entropy are the Rényi entropy introduced by Rényi (1960), and the Shannon entropy proposed by Shannon (1951). Rényi entropy for the HT-K-HL-G FoDs is

$$\begin{aligned} I_R(\omega) &= \frac{\log\left[\int_{-\infty}^{\infty} f_{HT-K-HL-G}^{\omega}(x;\Phi)dx\right]}{1-\omega} \\ &= \frac{\log\left[\sum_{s=0}^{\infty}\varepsilon_s e^{[(1-\omega)I_{REG}]}\right]}{1-\omega}, \omega \neq 1, \omega > 0, \end{aligned}$$

where

$$\begin{aligned} \varepsilon_s &= \left(2\alpha\theta^2\beta\right)^{\omega}\sum_{m,p,q,r=0}^{\infty}(-1)^{p+q+r+s}(1-\theta)^m\binom{\omega(\theta+1)+m}{m} \\ &\times \binom{\beta m+\omega(\beta\theta-1)}{p}\binom{\alpha p+\omega(\alpha-1)}{q}\binom{\alpha p+\omega(\alpha-1)+r-1}{r} \\ &\times \binom{q+r}{s}\left(\frac{\omega}{s+\omega}\right). \end{aligned}$$

and $I_{REG} = \left[\int_0^{\infty}\left(\frac{s}{\omega}+1\right)[g(x;\Phi)G^{\frac{s}{\omega}}(x;\Phi)]\right]^{\omega}$ is the Rényi entropy of the Expo-G distribution with parameter $(\frac{l}{\omega}+1)$. As a result, Rényi entropy of the HT-K-EHL-G FoDs stem directly from Rényi entropy of the Expo-G distribution. Visit the **web appendix** for detailed derivations.

3.6 Particular cases

This subsection presents some special cases of HT-K-HL-G FoDs by specifying the baseline cdf and pdf in Equations (10) and (12). The log-logistic and Weibull distributions are considered as baseline cdf in this section.

3.6.1 Heavy-Tailed Kumaraswamy Half-Logistic-G (HT-K-HL-Log-Logistic (HT-K-HL-LLoG) Distribution

Considering the log-logistic distribution with the cdf and pdf given by $G(x;\beta) = 1-\frac{1}{1+x^{\delta}}$ and $g(x;\delta) = \frac{\delta x^{\delta-1}}{(1+x^{\delta})^2}$ as baseline distribution, for $x, \delta > 0$, we have the HT-K-HL-LLoG distribution with cdf

$$F(x;\theta,\alpha,\beta,\delta) = 1-\left(\frac{\left[1-\left(\frac{x^{\delta}}{2+x^{\delta}}\right)^{\alpha}\right]^{\beta}}{1-(1-\theta)\left[1-\left(\frac{x^{\delta}}{2+x^{\delta}}\right)^{\alpha}\right]^{\beta}}\right)^{\theta}, \qquad (16)$$

and pdf

$$f(x;\theta,\alpha,\beta,\delta) = \frac{2\alpha\theta^2\beta\delta x^{\delta-1}}{(1+x^\delta)^2}\left(\frac{x^\delta}{2+x^\delta}\right)^{\alpha-1}\left[1-\left(\frac{x^\delta}{2+x^\delta}\right)^\alpha\right]^{\beta\theta-1} \times \left[1-(1-\theta)\left[1-\left(\frac{x^\delta}{2+x^\delta}\right)^\alpha\right]^\beta\right]^{-(\theta+1)}, \quad (17)$$

for $x,\theta,\alpha,\beta,\delta>0$.

3.6.2 Heavy-Tailed Kumaraswamy Half-Logistic-Weibull (HT-K-HL-W) Distribution

The HT-K-HL-W distribution is based on the Weibull distribution chosen as the baseline. Considering Weibull distribution with cdf and pdf given by $G(x;\omega)=1-\exp(-x^\omega)$ and $g(x;\omega)=\pi x^{\omega-1}\exp(-x^\omega)$, respectively, for $\omega,x>0$ as the baseline distribution, we have the HT-K-HL-W distribution with cdf

$$F(x;\theta,\alpha,\beta,\omega) = 1-\left(\frac{\left[1-\left(\frac{1-\exp(-x^\omega)}{1+\exp(-x^\omega)}\right)^\alpha\right]^\beta}{1-(1-\theta)\left[1-\left(\frac{1-\exp(-x^\omega)}{1+\exp(-x^\omega)}\right)^\alpha\right]^\beta}\right)^\theta$$

and pdf

$$f(x;\theta,\alpha,\beta,\omega) = \alpha\theta^2\beta\omega x^{\omega-1}\exp(-x^\omega)\left(\frac{1-\exp(-x^\omega)}{1+\exp(-x^\omega)}\right)^{\alpha-1} \times \left[1-\left(\frac{1-\exp(-x^\omega)}{1+\exp(-x^\omega)}\right)^\alpha\right]^{\beta\theta-1} \times \left[1-(1-\theta)\left[1-\left(\frac{1-\exp(-x^\omega)}{1+\exp(-x^\omega)}\right)^\alpha\right]^\beta\right]^{-(\theta+1)}, \quad (18)$$

for $\theta,\alpha,\beta,\omega,x>0$.

(a) HT-K-HL-LLOG density plot (b) HT-K-HL-W density plot

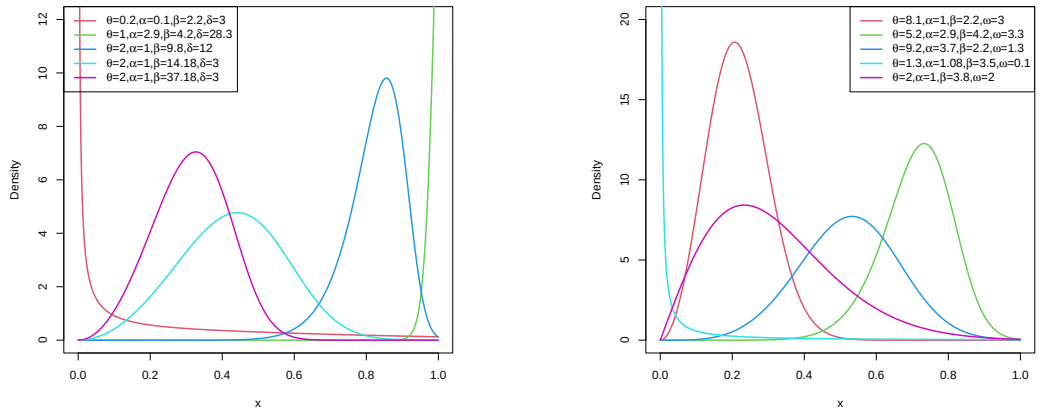

Figure 1: Density plots for selected parameter values

The graphical depictions presented in Figure [1] showcase the density plots associated with the HT-K-HL-LLoG and HT-K-HL-W distributions. The density plots show that both distributions can handle data that is positively skewed, negatively skewed and near symmetric shapes.

(a) HT-K-HL-LLOG hrf plot (b) HT-K-HL-W hrf plot

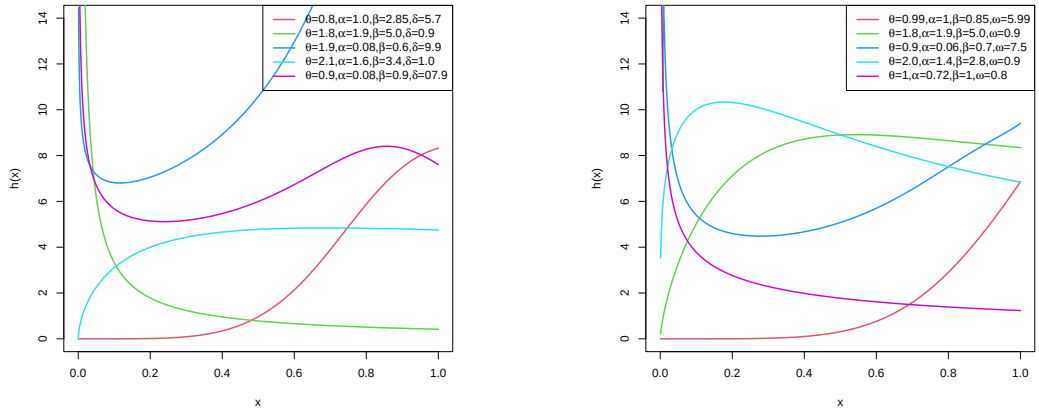

Figure 2: Some hazard rate patterns

The hrf plots illustrated in Figure [2] demonstrate the flexibility of the HT-K-HL-LLoG and HT-K-HL-W distributions in modeling diverse failure rate

behaviors. The results confirm that both distributions are capable of accommodating monotonic as well as non-monotonic hazard patterns, making them suitable for complex reliability and survival analysis applications. This adaptability underscores their robustness in capturing real-world lifetime data trends, which often exhibit varying failure rate characteristics over time.

(a) HT-K-HL-LLoG kurtosis

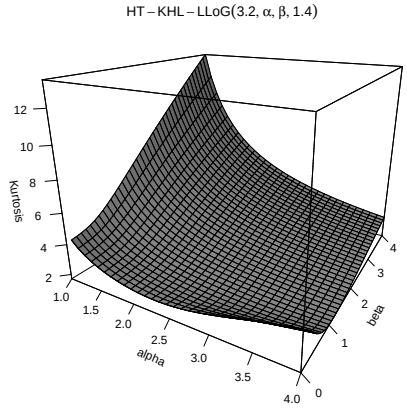

(b) HT-K-HL-LLoG skewness

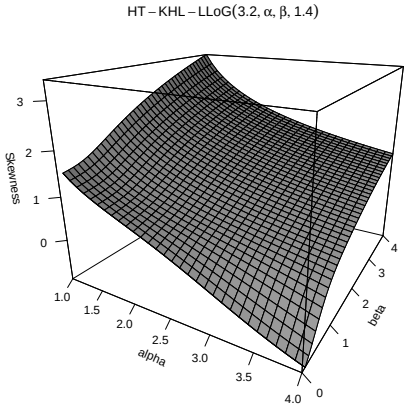

(c) HT-K-HL-W kurtosis

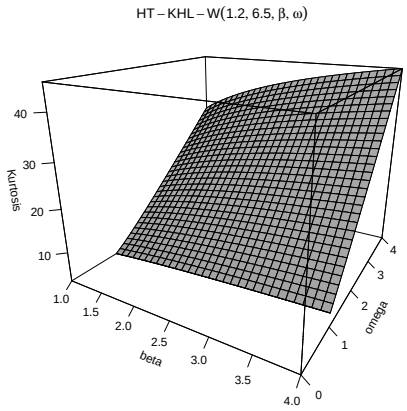

(d) HT-K-HL-W skewness

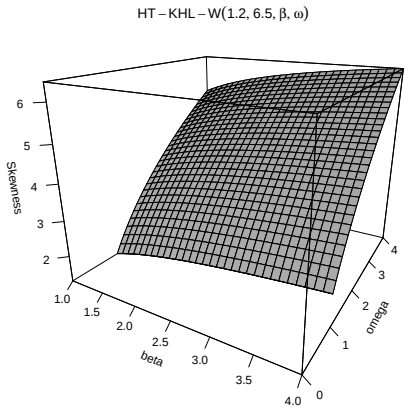

Figure 3: 3D visualisations of kurtosis and skewness for some selected parameter combinations

Analyzing 3D plots of skewness and kurtosis is essential for understanding how a distribution's shape and tail behavior change with different parameters, ensuring flexibility and accurate real-world data modelling. The 3D plots in

Figure [3]((a)-(d)) illustrate the kurtosis and skewness of the HT-K-HL-W and HT-K-HL-LLOG distributions. From the plots, it is evident that for the HT-K-HL-LLOG distribution, both kurtosis and skewness decrease as the parameters α and β increase, while keeping θ and δ constant. Similarly, for the HT-K-HL-W distribution, the kurtosis and skewness decrease with higher values of β and ω when α and θ are held fixed.

4 Actuarial Risk Measures

Actuarial risk measures are utilized by actuaries to assess and quantify market risk. This section investigates and evaluates several prominent risk measures, including Value at Risk (VaR), Tail Value at Risk (TVaR), Tail Variance (TV), and Tail Variance Premium (TVP). The analysis focuses on their theoretical foundations, computational methodologies, and applications in risk management.

4.1 VaR

VaR quantifies the maximum potential loss of an investment or business activity over a specified time horizon at a given confidence level, serving as a key metric for assessing downside risk. VaR_q, which is the u^{th} quantile for the HT-K-HL-G FoDs is calculated from

$$VaR_u = G^{-1}\left(\frac{\left(1-\left[\frac{(1-(1-\theta)u^{1/\theta})}{1-(1-\theta)u^{1/\theta}+u^{1/\theta}}\right]^{1/\beta}\right)^{1/\alpha}}{1+\left(1-\left[\frac{(1-(1-\theta)u^{1/\theta})}{1-(1-\theta)u^{1/\theta}+u^{1/\theta}}\right]^{1/\beta}\right)^{1/\alpha}}\right), \tag{19}$$

for $\alpha, \delta, b > 0$ and $0 \leq u \leq 1$ is the probability level.

4.2 TVaR

TVaR is a risk metric that expresses the expected value of losses following the occurrence of an event that exceeds a predefined probability threshold. For the HT-K-HL-G FoDs, TVaR can be calculated as follows:

$$\begin{aligned} TVaR_u &= E\left(X|X > x_u\right) = \frac{1}{1-u}\int_{VaR_u}^{\infty} xf(x;\theta,\alpha,\beta,\Phi)dx \\ &= \frac{1}{1-u}\sum_{l=0}^{\infty}\int_{VaR_u}^{\infty} x\Theta_{l+1}g_{l+1}(x;\Phi)dx, \end{aligned} \tag{20}$$

where Θ_{l+1} is as given in Equation (14) and $g_{l+1}(x;\Phi) = (l+1)G^l(x;\Phi)g(x;\Phi)$ represents the Expo-G pdf with power parameter $(l+1)$.

4.3 TV

TV is a risk measure that evaluates the conditional variance of losses exceeding the VaR at a specified probability threshold uu. It provides insight into the dispersion of extreme losses beyond the VaR threshold. The TV_u of the HT-K-HL-G FoDs is given by

$$\begin{aligned} TV_u &= E\left(X^2 \mid X > x_u\right) - (TVaR_u)^2 \\ &= \frac{1}{1-u}\int_{VaR_u}^{\infty} x^2 f(x;\theta,\alpha,\beta,\Phi)dx - (TVaR_u)^2, \end{aligned} \tag{21}$$

for $\theta, \alpha, \beta > 0$, Φ represents the parameter vector from the baseline distribution and $0 \leq u \leq 1$.

4.4 TVP

TVP is a risk measure used to assess the variability of extreme losses beyond a specified threshold, particularly in insurance and reinsurance contexts where high-severity risks are a key concern. The TVP of the HT-K-HL-G FoDs is expressed as

$$TVP_u = TVaR_u + \eta(TV_u), \tag{22}$$

where $0 < \eta < 1$. Equations (20) and (21) are substituted into Equation (22) to find the TVP of the HT-K-HL-G FoDs.

4.5 Quantitative Analysis of the Risk Measures

The numerical simulations in this subsection provide results for various risk measures. These risk measures are evaluated for the HT-K-HL-W distribution and compared to its non-nested models, the Kumaraswamy Weibull (KW) by Cordeiro, Ortega and Nadarajah (2010), heavy-tailed beta power transformed Weibull (HTBPTW) by Zhao et al. (2021) and the type I heavy-tailed-Weibull (TIHT-W) distributions by Zhao et al. (2020). The simulation results are obtained using the following methodology:

(1) stochastic samples of size 100 are generated from each distribution, and the parameters are estimated using MLE technique.

(2) a total of 1000 iterations are performed to calculate the risk measures for these distributions.

The results of the numerical analysis conducted on risk measures are displayed in Table [1]. Higher values of the risk metrics indicate distributions characterized by heavier tails. Among the analyzed distributions, the HT-K-HL-W

distribution shows a heavier tail. This suggests that the HT-K-HL-W distribution is a suitable choice for modeling datasets that display heavy-tailed characteristics.

Table 1: Results of Risk Metrics Simulations

Significance level	Risk measure	0.75	0.80	0.85	0.90	0.95	0.99
HT-K-HL-W($\theta = 0.5, \alpha = 2.0, \beta = 1.0, \omega = 0.3$)	VaR	2.6991	4.3324	7.3465	13.8215	33.2662	148.2096
	TVaR	35.7310	43.7840	56.4330	79.410	136.4700	402.0016
	TV	14597	17923	23257	33301	60080	209672
	TVP	11714	14382	18662	26721	48201	168140
KW($a = 1.0, b = 1.0, \alpha = 1.0, \beta = 1.0$)	VaR	1.3711	1.5901	1.8717	2.2675	2.9409	4.4916
	TVaR	2.3453	2.5625	2.8419	3.2347	3.9034	5.4446
	TV	0.9353	0.9322	0.9284	1.0463	1.5237	2.9644
	TVP	3.0935	3.3082	3.5846	4.0717	5.1224	7.8161
HTBPTW($\alpha = 1.0, \gamma = 1.0, \beta = 0.5$)	VaR	1.2748	1.6494	2.1387	2.8612	4.2184	8.0695
	TVaR	3.5711	3.9517	4.4779	5.2832	6.8298	11.2378
	TV	3.5679	4.0370	4.6594	5.5916	7.3412	12.6287
	TVP	6.4254	7.1813	8.2054	9.7565	12.7028	21.3408
TIHT-W($\omega = 0.3, \theta = 0.5, \gamma = 1.2$)	VaR	1.1043	1.7213	2.8073	4.9944	10.9259	39.2838
	TVaR	9.1976	11.1505	14.1309	19.3173	31.2657	77.9072
	TV	374.3400	448.8400	562.8900	763.4500	1238.5800	3257.3700
	TVP	308.6700	370.2300	464.4500	630.0800	1022.1300	2683.8000

5 Estimation

We employ the maximum likelihood estimation (MLE) technique to derive parameter estimates for the HT-K-HL-G FoDs.

5.1 Maximum likelihood estimation

Suppose we have random variables X_i following a HT-K-HL-G FoDs, and let $\Lambda = (\theta, \alpha, \beta, \Phi)^T$ represent the model parameters vector. In this context, the log-likelihood $\ell(\Lambda)$ for a sample of size n can be represented as

$$\begin{aligned}
\ell(\Lambda) &= n\ln(2) + n\ln(\alpha) + 2n\ln(\theta) + n\ln(\beta) + \sum_{i=1}^{n} \ln g(x_i;\Phi) \\
&+ (\alpha-1)\sum_{i=1}^{n} \ln\left(\frac{G(x_i;\Phi)}{1+\bar{G}(x_i;\Phi)}\right) \\
&+ (\beta\theta-1)\sum_{i=1}^{n} \ln\left[1-\left(\frac{G(x_i;\Phi)}{1+\bar{G}(x_i;\Phi)}\right)^{\alpha}\right] \\
&- (\theta+1)\sum_{i=1}^{n} \ln\left[1-(1-\theta)\left(1-\left(\frac{G(x_i;\Phi)}{1+\bar{G}(x_i;\Phi)}\right)^{\alpha}\right)^{\beta}\right]. \quad (23)
\end{aligned}$$

The system of nonlinear equations $\left(\frac{\partial\ell}{\partial\theta}, \frac{\partial\ell}{\partial\alpha}, \frac{\partial\ell}{\partial\beta}, \frac{\partial\ell}{\partial\Phi_k}\right)^T = \mathbf{0}$ can be solved numerically using the Newton-Raphson iteration method to estimate the parameters

θ, α, β, and Φ_k. The maximum likelihood estimation and related computations may be conveniently performed through computational statistical packages, including but not limited to R, MATLAB, or Python-based numerical optimization tools. The partial derivatives of the log-likelihood function $\ell(\Lambda)$ are given in **web appendix**.

6 Simulations

To evaluate the efficiency of the MLEs, a simulation study was carried out. The findings from the simulation are presented in Table 2. We simulated for n= 25, 80, 160, 250, 500 and 1000 for N=3000 from the HT-KHL-W distribution. The average bias (AvBIAS) and root mean square error (RMSEr) for an estimated parameter, say $(\hat{\theta})$, are computed using the following formulae

$$AvBIAS(\hat{\theta}) = \frac{\sum_{j=1}^{N} \hat{\theta}_j}{N} - \theta, \quad \text{and} \quad RMSEr(\hat{\theta}) = \sqrt{\frac{\sum_{j=1}^{N} (\hat{\theta}_j - \theta)^2}{N}},$$

respectively. Based on the findings presented in Table 2, it is apparent that the mean values exhibit a high degree of proximity to the true parameter values. Moreover, as the sample size increases, both the RTMSEr and the AvBIAS tend to approach zero across all parameters. This shows that the HT-KHL-W distribution produces efficient parameters estimates.

Table 2: Results of Monte Carlo Simulations for the HT-KHL-W Distribution: Mean, RMSEr, and AvBIAS

		$\theta = 1.0, \alpha = 3.5, \beta = 0.2, \omega = 3.5$			$\theta = 1.2, \alpha = 0.02, \beta = 1.0, \omega = 3.5$		
	n	Mean	RMSEr	AvBIAS	Mean	RMSEr	AvBIAS
	25	1.3500	1.3316	0.3500	1.4870	1.4040	0.4870
	80	1.1106	0.4608	0.1106	1.2704	0.6941	0.2804
α	160	1.0978	0.4155	0.0978	1.2719	0.5222	0.2719
	250	1.0810	0.4003	0.0810	1.2389	0.4066	0.2389
	500	1.0112	0.2505	0.0112	1.2373	0.3827	0.2373
	1000	1.0150	0.1801	0.0150	1.2010	0.0127	-0.1910
	25	3.9648	1.9495	1.3648	0.1043	0.7378	0.0843
	80	3.7253	1.7770	0.1253	0.0331	0.0532	0.0131
δ	160	3.5947	1.3580	0.0953	0.0283	0.0265	0.0083
	250	3.5401	1.2755	0.0699	0.0253	0.0174	0.0053
	500	3.5111	0.7669	0.0311	0.0235	0.0137	0.0035
	1000	3.5007	0.5487	0.0293	0.0218	0.0069	0.0018
	25	0.4838	0.3970	0.7338	1.4167	0.6619	0.3067
	80	0.3042	0.1386	0.0542	1.2109	0.5984	0.2109
b	160	0.2812	0.0847	0.0312	1.0843	0.2789	0.0843
	250	0.2743	0.0722	0.0243	1.0581	0.1996	0.0581
	500	0.2380	0.0467	0.0180	1.0315	0.1297	0.0315
	1000	0.2101	0.0295	0.0101	1.0153	0.0767	0.0153
	25	3.8499	1.3139	0.3499	3.1724	0.8122	-0.3276
	80	3.7569	0.7833	0.2569	3.3468	0.4577	-0.1532
β	160	3.6503	0.5788	0.1503	3.4090	0.3084	-0.0910
	250	3.6175	0.4816	0.1175	3.4275	0.2231	-0.0725
	500	3.5435	0.3754	0.0435	3.4510	0.1602	-0.0490
	1000	3.5110	0.0948	0.0090	3.4687	0.0969	-0.0313

7 Applications

The HT-K-HL-W distribution is applied to real-world data and compared with various non-nested models, including established heavy-tailed distributions, in order to assess its performance. A comparison was made between the HT-K-HL-W model and six other non-nested models namely, the odd exponentiated half logistic Burr XII (OEHLBXII) by Aldahlan and Afify (2018), the exponential Lindley odd log-logistic Weibull (ELOLLW) by Korkmaz et al. (2018), the type I heavy-tailed-Weibull (TIHT-W) by Zhao et al. (2020), the heavy-tailed beta power transformed Weibull (HTBPTW) by Zhao et al. (2021), the Kumaraswamy Weibull (KW) by Cordeiro, Ortega and Nadarajah (2010) and the the exponentiated half logistic Weibull Poisson (EHLWP) by Chipepa et al. (2022). The pdfs of the distributions used in the comparisons are provided in the **web appendix**.

The analysis incorporated a set of goodness-of-fit (GoF) statistics, encompassing the following measures: -2 log-likelihood ($-2\log(L)$), Akaike Information Criterion ($AIC = 2p - 2\log(L)$, Consistent Akaike Information Criterion ($CAIC = AIC + 2\frac{p(p+1)}{n-p-1}$), Bayesian Information Criterion ($BIC = p\log n - 2\log(L)$ (where n is the number of observed parameters, while the

number of calculated parameters is p) and the Kolmogorov-Smirnov (K-S) test statistics. The statistical analysis aimed at identifying the optimal model for the given dataset by evaluating various GoF criteria. The selected model was chosen based on the highest p-value for the K-S statistic, along with the lowest values for other statistical measures. The parameters of the models were estimated using the nonlinear minimization function (nlm) in R statistical software. Each parameter estimate is reported with its corresponding standard error (SE), presented in parentheses. To assess model adequacy, several diagnostic plots were generated, including fitted density curves, the empirical cumulative distribution function (ECDF), the Kaplan-Meier (K-M) survival curve, and the total time on test (TTT) plot. These visualizations provide further validation of the model's fit to the observed data.

7.1 Windshields failure times data

The following virtually symmetric dataset, previously examined by Murthy and Xie (2004) and later revisited by Muhammad, Muhammad, and Alya Al (2021), comprises failure times (in arbitrary units) of windshield specimens: The values are: 0.04, 0.3, 0.31, 0.557, 0.943, 1.07, 1.124, 1.248, 1.281, 1.281, 1.303, 1.432, 1.48, 1.51, 1.51, 1.568, 1.615, 1.619, 1.652, 1.652, 1.757, 1.795, 1.866, 1.876, 1.899, 1.911, 1.912, 1.9141, 0.981, 2.010, 2.038, 2.085, 2.089, 2.097, 2.135, 2.154, 2.190, 2.194, 2.223, 2.224, 2.23, 2.3, 2.324, 2.349, 2.385, 2.481, 2.610, 2.625, 2.632, 2.646, 2.661, 2.688, 2.823, 2.89, 2.9, 2.934, 2.962, 2.964, 3, 3.1, 3.114, 3.117, 3.166, 3.344, 3.376, 3.385, 3.443, 3.467, 3.478, 3.578, 3.595, 3.699, 3.779, 3.924, 4.035, 4.121, 4.167, 4.240, 4.255, 4.278, 4.305, 4.376, 4.449, 4.485, 4.570, 4.602, 4.663, 4.694.

18

Table 3: Estimation and Statistical Analysis of Parameters on Windshields Data

									GoF Statistics	
Distribution	Estimates and SEs				-2log(L)	AIC	CAIC	BIC	K−S	p−value
	θ	α	β	ω						
HT-K-HL-W	0.3714	21.5230	1.08×10^{7}	0.1007	171.2904	179.2904	179.7723	189.1997	0.0538	0.9607
	(0.1637)	(0.8911)	(1.07×10^{-7})	(8.52×10^{-3})						
	α	λ	a	b						
OEHLBXII	0.8978	0.0471	1.1636	2.1854	330.9621	338.9621	339.4440	348.8714	0.0847	0.5528
	(0.2766)	(0.0568)	(0.1807)	(0.7101)						
	b	λ	θ	γ						
ELLOW	2.0178	0.6170	0.6399	1.8747	271.8209	279.8209	280.3028	289.7302	0.0592	0.9037
	(0.2576)	(0.3953)	(0.6101)	(0.2543)						
	ω	θ	γ							
TIHT-W	2.4050	21.0910	1.81×10^{-4}		275.0385	281.0385	281.3242	288.4705	0.0579	0.9143
	(4.32×10^{-9})	(3.47×10^{-10})	(2.00×10^{-5})							
	α	γ	β							
HTBPTW	2.0090	0.1562	2.2713		272.8443	278.8443	279.1300	286.2763	0.0612	0.8835
	(0.2597)	(0.0609)	(0.3798)							
	a	b	α	β						
KW	0.9852	1.11×10^{3}	0.0176	2.3906	274.1796	282.1796	282.6616	292.0890	0.0553	0.9262
	(0.5888)	(5.12×10^{-5})	(4.41×10^{-3})	(1.4264)						
	α	β	δ	θ						
EHLWP	1.7253	4.21×10^{-3}	1.3654	374.5700	274.1879	282.1879	282.6698	292.0972	0.0576	0.9201
	(0.7034)	(0.0266)	(1.3992)	(1.69×10^{-3})						

Table [3] presents the maximum likelihood estimates (MLEs) of the parameters for the HT-K-HL-Weibull (HT-K-HL-W) distribution, derived from windshield failure data through numerical optimization of the log-likelihood function specified in Equation (23). The associated SEs are reported parenthetically. The 95% asymptotic confidence intervals for the parameters are as follows: $\theta \in [0.3714 \pm 0.3209$, $\alpha \in [21.5230 \pm 1.7466$, $\beta \in [\ 1.08 \times 10^{7} \pm 2.09 \times 10^{-7}]$ and $\omega \in [0.1007 \pm 0.0167]$, respectively. Based on GoF metrics evaluated on windshield data, the HT-K-HL-W model demonstrates superior performance compared to the non-nested competing models under consideration.

(a) Estimated density (b) Empirical and estimated cdfs

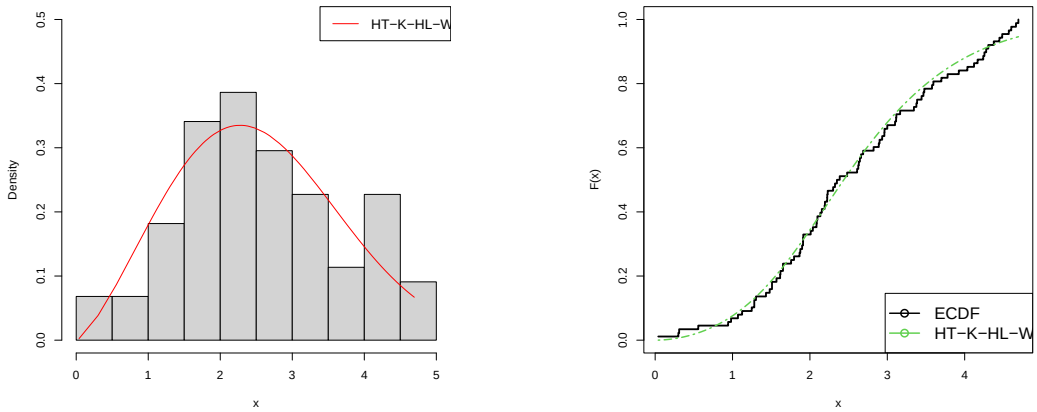

Figure 4: Fitted density and empirical and estimated cdfs

As evidenced in Figure [4], the HT-K-HL-W model provides an excellent approximation of the windshields data, showing strong concordance across both the histogram representation and empirical cumulative distribution curve.

(a) K-M survival curve (b) TTT-scaled plot

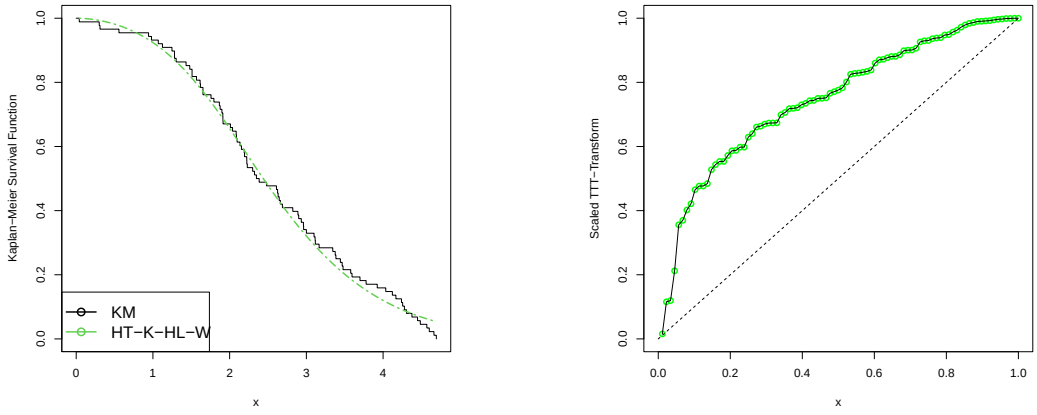

Figure 5: Fitted density and empirical and estimated cdfs

Figure [5] illustrates the efficacy of the HT-K-HL-W distribution in modeling both the survival behavior and underlying failure processes of windshield data. The strong concordance between the observed and fitted K-M survival functions demonstrates the model's estimation precision, while the consistently

rising pattern in the TTT-scaled plot empirically supports the inclusion of time-varying degradation effects in the model's formulation.

7.2 Relief times data

The dataset comprises right-skewed lifetime data, as examined by Muhammad, Muhammad, and Alya Al (2021). This dataset encapsulates the analgesic relief durations (measured in minutes) for a cohort of 20 patients. The recorded values are as follows: The values are: 1.1, 1.4, 1.3, 1.7, 1.9, 1.8, 1.6, 2.2, 1.7, 2.7, 4.1, 1.8, 1.5, 1.2, 1.4, 3, 1.7, 2.3, 1.6, 2.

Table 4: Estimation and Statistical Analysis of Parameters on Relief Times Data

									GoF Statistics	
Distribution	Estimates and SEs				-2log(L)	AIC	CAIC	BIC	K−S	p−value
	θ	α	β	ω						
HT-K-HL-W	3.5479	20.7520	6.99×10^{4}	0.1943	15.7049	23.7049	26.3716	27.6879	0.1679	0.6256
	(1.7434)	(0.1465)	(3.59×10^{-5})	(0.0372)						
	α	λ	a	b						
OEHLBXII	0.6220	0.2263	121.5200	0.0185	46.6118	54.6118	57.2785	58.5948	0.1852	0.4987
	(0.2348)	(0.2668)	(0.1807)	(7.20×10^{-3})						
	b	λ	θ	γ						
ELLOW	2.1091	0.5742	0.5705	2.7870	41.1728	49.1728	51.8395	53.1557	0.1849	0.5006
	(0.1451)	(0.0689)	(0.0249)	(0.4273)						
	ω	θ	γ							
TIHT-W	3.3121	3.2607	0.0093		38.8809	44.8809	46.3810	47.8682	0.1722	0.5950
	(0.5148)	(0.4549)	(0.0149)							
	α	γ	β							
HTBPTW	2.7870	0.1216	1.0012		41.1728	47.1728	48.6728	50.1600	0.1850	0.5005
	(0.4273)	(0.0563)	(1.0373)							
	a	b	α	β						
KW	87.6220	1.05×10^{3}	164.7500	0.1616	38.6368	46.6368	49.3038	50.6198	0.1875	0.4828
	(1.47×10^{-6})	(1.90×10^{-8})	(3.46×10^{-7})	(2.11×10^{-3})						
	α	β	δ	θ						
EHLWP	0.1842	8.788	1.96×10^{4}	6.9736	32.2025	40.2025	42.8722	44.1884	0.1711	0.5622
	(0.0478)	(0.1758)	(9.49×10^{-6})	(3.1654)						

Table [4] displays the MLEs of the unknown parameters for the HT-K-HL-W distribution, which were obtained from relief times data. The asymptotic confidence intervals at 95% confidence level for the model parameters are: $\theta \in [3.5479 \pm 3.4170$, $\alpha \in [20.7520 \pm 2.83\times10^{-3}]$, $\beta \in [\ 6.99\ \times10^{4} \pm 7.03\ \times10^{-5}]$ and $\omega \in [0.1943 \pm 0.0729]$, respectively. Consequently, the HT-K-HL-W model out-performs the non-nested models that were considered according to the GoF obtained on relief times data.

(a) Fitted density (b) Empirical and estimated cdfs

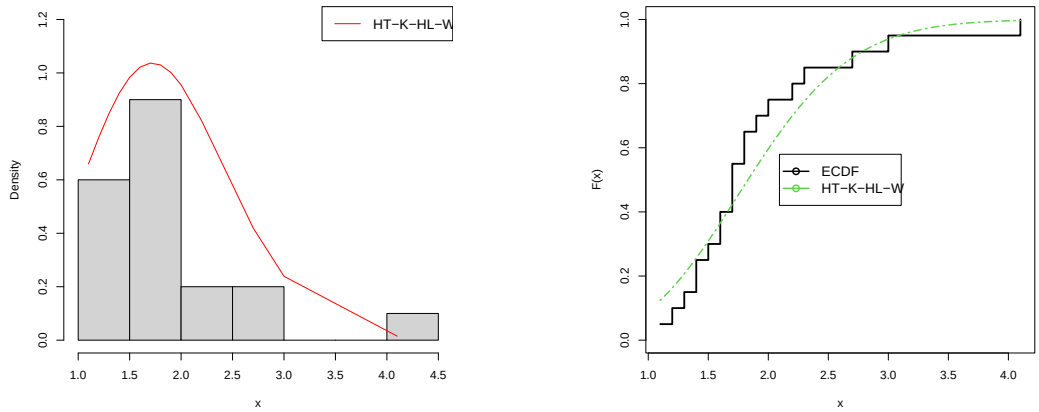

Figure 6: Fitted density and empirical and estimated cdfs

Figure [6] demonstrates that the HT-K-HL-W model closely approximates the relief times data, with a high degree of similarity visible in both the histogram and the empirical cumulative distribution function.

(a) K-M survival curve (b) TTT-scaled plot

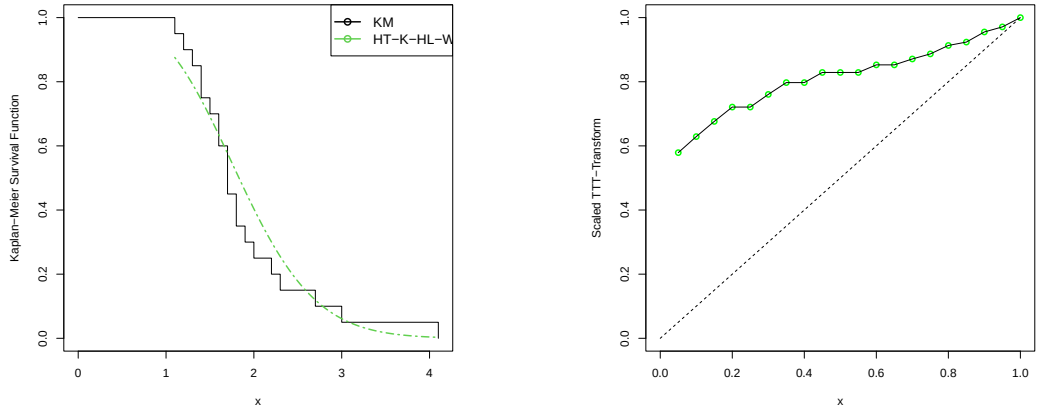

Figure 7: Fitted density and empirical and estimated cdfs

Figure [7] reveals an excellent fit between the HT-K-HL-W model and the relief times data, with remarkable consistency in the K-M curve. The trend in the TTT plot suggests that the data follows an increasing hazard rate pattern.

8 Concluding Remarks

In summary, this study presents the Heavy-Tailed Kumaraswamy Half-Logistic-G (HT-K-HL-G) FoDs as a robust statistical framework for modeling heavy-tailed phenomena. A comprehensive investigation of the HT-K-HL-G FoDs was conducted, including derivation of key statistical properties and actuarial risk measures. Through empirical validation, the HT-K-HL-Weibull (HT-K-HL-W) distribution, a special member of the HT-K-HL-G family, was shown to outperform competing non-nested models in capturing diverse data behaviors. The superior flexibility and fit of the proposed distributions underscore their high practical significance in critical fields such as survival analysis, reliability engineering, and actuarial science, where precise modeling of heavy-tailed data is essential for risk quantification, predictive accuracy, and data-driven decision-making. These advancements position the HT-K-HL-G FoDs as a transformative tool for enhancing statistical modeling in real-world applications characterized by extreme-valued data.

To access the appendix, kindly click on the link provided below:
`https://drive.google.com/file/d/1YpkgdmPB58YODZz09j5xYfTWmaQhM-sw/view?usp=sharing`

References

Aldahlan, M. & Afify, A. Z. (2018). The odd exponentiated half-logistic Burr XII distribution. *Pakistan Journal of Statistics and Operation Research*, **14**(2):305-317.

Chipepa, F., Oluyede, B., Chamunorwa S., Makubate B. & Zidana, C. (2022). The exponentiated half logistic-generalized-G power series class of distributions: Properties and applications. *Journal of Probability and Statistical Scienc*e, **20**(1):21-40.

Cordeiro G. M., Alizadeh M. & Diniz Marinho P. R. (2016). The type I half-logistic family of distributions. *Journal of Statistical Computation and Simulation*, **86**(4):707–728.

Cordeiro G. M & de Castro J. (2011). A new family of generalized distributions. *Journal of Statistical Computation and Simulation*, **81**:883–893.

Cordeiro G. M., Ortega E. M. & Nadarajah S. (2010). The Kumaraswamy Weibull distribution with application to failure data. *Journal of the Franklin Institute*, **7**(8):1399–1429.

Handique L., Chakraborty S. & Hamedani G. G. (2017). The Marshall-Olkin-Kumaraswamy-G family of distributions. *Journal of Statistical Theory and Applications*, **16**(4):427–447.

Ishaq A. I., Panitanarak U., Abiodun A. A., Suleiman A. A. & Daud H. (2024). The generalized odd Maxwell-Kumaraswamy distribution: Its properties and applications. *Contemporary Mathematics*, **5**(1):711–742.

Korkmaz, M. C., Yousof, H. M, & Hamedani, G. G. (2018). The exponential Lindley odd log-logistic-G family: Properties, characterizations and applications. *Journal of Statistical Theory and Applications*, **17**(3), 554-571.

Muhammad A., Muhammad Z. I. & Alya Al M. (2021). A comprehensive review of datasets for statistical research in probability and quality control. *Journal of Mathematics and Computer Science*, **11**(3):3663 3728.

Murthy D. N, P. & Xie R. J. (2004). Weibull models. *John Wiley & Sons Inc., Hoboken.*

Nkomo W., Oluyede B. & Chipepa F. (2025). Topp-Leone type I heavy-tailed-G power series class of distributions: Properties, risk measures, and applications. *Statistics, Optimization and Information Computing*, **13**(1):88–110.

Nkomo W., Oluyede B. & Chipepa F. (2025). The New Topp-Leone-Heavy-Tailed Type II Exponentiated Half Logistic-G Family of Distributions: Properties, Actuarial Measures, with Applications to Censored Data. *Pakistan Journal of Statistics and Operation Research*, **21**(2):213–236.

Oluyede, B. & Moakofi, T. (2023). The Gamma-Topp-Leone-type II-exponentiated half logistic-G family of distributions with applications. *Stats*, **6**, 706–733.

Rényi, A. (1960). On Measures of Entropy and Information. Proceedings of the Fourth Berkeley Symposium on Mathematical Statistics and Probability. *University of Carlifonia Press, Berkeley and Los Angeles*, **1**, 547-561.

Shannon, C. E. (1950). Prediction and Entropy of Printed English. *The Bell System Technical Journal*, **30**, 50-64.

Zhao, J., Ahmad, Z., Mahmoudi, E., Hafez, E. H. & Mohie El-Din, M. M. (2021). A new class of heavy-tailed distributions: Modeling and simulating actuarial measures, *Hindawi*, 1-18.

Zhao, W., Khosa, S. K., Ahmad, Z., Aslam M. & Afify, A. Z. (2020). Type-I heavy-tailed family with applications in medicine, engineering and insurance. *PLoS ONE*, **15**(8), 63-79.